Compensation of the Impact of Interference Mitigation by Pulse Blanking in OFDM Systems

Sinja Brandes, Ulrich Epple, and Michael Schnell
German Aerospace Center (DLR), Oberpfaffenhofen, Germany
Institute of Communications and Navigation
email: {sinja.brandes, ulrich.epple, michael.schnell}@dlr.de

***Abstract*—When pulsed interference is mitigated by means of pulse blanking, interference is reduced significantly. However, at the same time certain fractions of the useful orthogonal frequency-division multiplexing (OFDM) signal are erased. Consequently, only moderate improvements are achieved with pulse blanking. When representing the pulse blanking operation as multiplication with a rectangular window exhibiting notches at the positions where blanks are inserted, it becomes obvious, that pulse blanking mainly leads to inter-carrier interference (ICI). In this paper, the compensation of the impact of pulse blanking is proposed by reconstructing and subtracting ICI. The required shape of the subcarrier spectra is derived from the pulse blanking window. For an estimation of the transmitted data symbols and the channel coefficients of each subcarrier an iterative receiver structure is proposed. Simulation results at hand of a realistic interference scenario show that with perfect channel estimation and known data symbols the impact of pulse blanking can be reduced to a small loss in signal-to-noise ratio resulting from the energy loss due to erasing a certain fraction of the OFDM signal. With real channel estimation and estimated data symbols, the interference-free case is approached by 2.8 dB after only three iterations.**

I. Introduction

To overcome the contradiction of spectral scarcity on the one hand and the ever-growing demand for more bandwidth and higher data rates on the other hand, spectral efficiency has to be increased. A promising approach is the co-existence of two systems in the same frequency band.

This concept has recently been proposed for the future L-band Digital Aeronautical Communications System (L-DACS) [1]. The aeronautical L-band (960-1164 MHz) is mainly subdivided into channels with 1 MHz bandwidth each and used by the distance measuring equipment (DME) or the military tactical air navigation (TACAN) system, both being aeronautical navigation systems based on radar technology. As depicted in Fig. 1, the gap between two adjacent DME channels that has a bandwidth of approximately 500 kHz is intended to be used by an OFDM system referred to as L-DASC1. This inlay deployment concept and the small separation of the two systems in frequency pose a challenge to the suppression of mutual interference between the two systems. Due to the smaller transmit (Tx) power of the OFDM system, it is sufficient to reduce out-of-band radiation by conventional methods such as Tx windowing. However, the OFDM system is exposed to interference from DME and other L-band systems, all being characterised by high power and large bandwidth.

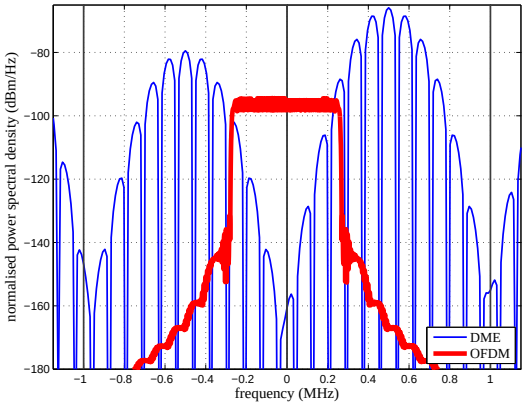

Fig. 1. Illustration of inlay concept: OFDM spectrum in gap between two adjacent DME channels.

A common approach for mitigating the impact of interference from DME or other sources of pulsed interference is pulse blanking [2]. Pulse blanking suffers from the drawback that it impairs the desired signal. This is a serious problem especially in OFDM systems since it leads to ICI that significantly degrades performance such that all in all, only moderate performance improvements are achievable with pulse blanking. In this paper, a method for compensating the impact of pulse blanking on the OFDM signal is proposed.

The remainder of this paper is organized as follows. In Section II, the used interference model and the expected impact of interference on the OFDM signal are described. After introducing pulse blanking for interference mitigation and analyzing the impact of pulse blanking on the desired signal, the compensation of the impact of pulse blanking is proposed in Section IV. Special emphasis is put on the estimation of Tx data and channel coefficients as well as on the re-optimization of the pulse blanking threshold. The performance of the proposed method is demonstrated with simulations using a realistic interference scenario. Finally, conclusions are drawn in Section VI.

II. Interference Model

The DME signal consists of pairs of Gaussian-shaped pulses, where each pulse has a duration of 3.5 μs between

the 50% amplitude points on leading and trailing edges of the pulse envelope. Depending on the mode, the interval between the two pulses of a pulse pair ranges from 12 to 36 μs. To model the impact of interference as realistically as possible, the radio frequency filter at the OFDM receiver (Rx) is taken into account. As the sampling frequency of the OFDM systems violates the sampling theorem for the interference signal, an anti-aliasing filter in combination with four-times over-sampling is introduced. Hence, interference from DME stations in channels at frequency offsets equal to or larger than ± 1.5 MHz is negligible.

In the two relevant channels at ± 0.5 MHz offset to the OFDM system, the interference signals from multiple DME stations superimpose. One DME station may transmit up to 3600 pulse pairs per second (ppps). In a typical interference scenario four DME stations occur in both adjacent channels producing a total pulse rate as high as 14400 ppps. Modelling the starting times of the pulse pairs as a Poisson process, the probability that an OFDM symbol is hit by DME interference is given by the complementary probability of the event that no interference occurs within an OFDM symbol, i.e.

$$P_{\text{hit}} = 1 - e^{-\eta(T_O + 3.5\mu\text{s})} \tag{1}$$

with T_O denoting the duration of an OFDM symbol which is 96 μs for the considered OFDM system. Note, the observed interval has to be extended by the duration of one pulse. The intensity η of the Poisson process is determined by the number of pulses which is $2 \cdot 14400$ pulses per second in the regarded example. With the given parameters, the probability that an OFDM symbol is hit is 94%. The probability that one OFDM symbol is hit by two pulses is as high as 23%.

Taking into account the sampling rate of the considered OFDM system that is 1.5 μs or 0.375 μs without or with four times over-sampling, about three or 12 samples of the desired signal are affected when a DME pulse occurs, respectively. Due to the high duty cycle and high power, DME interference has a severe impact on the performance of the OFDM system and hence has to be mitigated.

III. Interference Mitigation by Pulse Blanking

A well-known approach to combat pulsed interference is pulse blanking (PB), which has already been applied to DME interference in the E5- and L5-bands used by satellite navigation systems [2] and to impulsive noise in OFDM systems [3].

When the amplitude of the over-sampled Rx signal exceeds the threshold T^{PB} the corresponding samples are blanked. Let $r_p^{\text{ov}}[k]$ denote samples of the pth over-sampled OFDM symbol of the Rx frame containing P OFDM symbols. One OFDM symbol is represented by VN time samples with V and N denoting the over-sampling factor and the FFT length, respectively. The Rx signal after PB $r_p'^{\text{ov}}[k]$ yields

$$r_p'^{\text{ov}}[k] = \begin{cases} r_p^{\text{ov}}[k] & |r_p^{\text{ov}}[k]| \leq T^{\text{PB}} \\ 0 & |r_p^{\text{ov}}[k]| > T^{\text{PB}} \end{cases} \tag{2}$$
$$k = 0, \ldots, VN-1,\ p = 0, \ldots, P-1.$$

On the one hand, the threshold T^{PB} has to be chosen as small as possible such as to keep the interference power remaining after PB at a minimum. On the other hand, since also the useful OFDM signal is affected by PB, T^{PB} has to be set as high as possible to minimize the impact on the useful OFDM signal and the resulting performance degradation. Hence, the threshold T^{PB} is a crucial parameter that has to be determined as a trade-off between the achievable reduction of interference power and the impact on the desired OFDM signal. In [3], [4], the signal-to-noise-and-interference ratio (SINR) after PB is employed as optimization criterion for T^{PB}.

In OFDM systems, the number and position of samples to be blanked cannot easily be derived from the entire Rx signal, since even the useful signal exhibits peaks that may be falsely identified as pulses. Therefore, the detection of pulses in the Rx signal based on a correlation of the Rx signal with a known interference pulse has been proposed in [5]. Compared to PB based on the perfectly known interference signal, in most cases the same number of samples is blanked in the Rx signal. Thus, in the following, perfect pulse detection based on the actual interference signal is assumed.

IV. Compensation of Pulse Blanking Impact

PB reduces interference power, hence improving the performance of the OFDM system. However, at the same time certain parts of the desired OFDM signal are erased resulting in a performance degradation. In total, only moderate performance improvements are achieved with PB even when the threshold T^{PB} is chosen optimally. The PB impact on the useful signal can be diminished by exploiting special properties of OFDM signals as explained in the following.

A. Impact of Pulse Blanking

The PB impact on the OFDM signal can be determined exactly when representing PB as a windowing operation. The window function is a rectangular window that exhibits notches at those positions where the Rx signal is blanked. Recalling that the shape of the window determines the spectrum of the OFDM subcarriers, the subcarrier spectra can be determined and the distortion induced by PB is identified as ICI. ICI can easily be reduced by subtracting the known impact of all other subcarriers from the considered subcarrier as applied for example for reducing ICI in orthogonal frequency-division multiple-access (OFDMA) systems induced by frequency offsets [6].

As the number and positions of notches varies from OFDM symbol to OFDM symbol, the windowing function $w_p^{\text{PB}}[k]$ has to be defined for each OFDM symbol individually. As illustrated in Fig. 2, the lower and upper boundaries of the notches are denoted by $B_{p,b}^{\text{l}}$ and $B_{p,b}^{\text{u}}, b = 0, \ldots, N_{\text{B},p} - 1$, where $N_{\text{B},p}$ is the number of notches in the pth OFDM symbol. Hence, the windowing function $w_p^{\text{PB}}[k]$ for the pth OFDM

symbol with $p = 0, \ldots, P-1$ yields

$$w_p^{\mathrm{PB}}[k] = \begin{cases} 1 & 0 \le k \le B_{p,0}^{\mathrm{l}}, \\ & B_{p,0}^{\mathrm{u}} \le k \le B_{p,1}^{\mathrm{l}}, \ldots, \\ & B_{p,N_{\mathrm{B},p}-1}^{\mathrm{u}} \le k \le VN-1, \\ 0 & \text{otherwise} \end{cases} \quad (3)$$

With (3), the time domain signal of the pth OFDM symbol after PB is given by

$$r_p'^{\mathrm{ov}}[k] = w_p^{\mathrm{PB}}[k] \cdot r_p^{\mathrm{ov}}[k], \quad k = 0, \ldots, VN-1,\ p = 0, \ldots, P-1, \quad (4)$$

which is equivalent to the definition of the PB operation from (2).

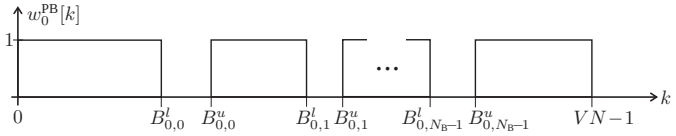

Fig. 2. Pulse blanking window, $p = 0$.

B. Reduction of ICI

For evaluating and compensating ICI, the spectra of the individual subcarriers after PB have to be derived. In OFDM, the subcarrier spectrum is determined by the window that extracts an OFDM symbol from the data stream. In contrast to the conventional rectangular window of length corresponding to the length of one OFDM symbol, after PB, the PB window as defined in (3) has to be taken into account. The time domain carrier signal $s_{p,\nu}[k]$ on the νth subcarrier of the pth OFDM symbol equals

$$s_{p,\nu}[k] = w_p^{\mathrm{PB}}[k] \cdot e^{j2\pi\nu k/V/N},\ k = 0, \ldots, VN-1. \quad (5)$$

The spectrum of the νth subcarrier can be calculated by Fourier transforming (5) to the frequency domain. Taking into account V-times over-sampling, the νth subcarrier spectrum $S_{p,\nu}[n]$ yields

$$\begin{aligned} S_{p,\nu}[n] &= \mathrm{DFT}\{s_{p,\nu}[k]\} \quad (6) \\ &= \sum_{k=0}^{B_0^{\mathrm{l}}} e^{-jk(\Omega-\Omega_\nu)} + \sum_{b=0}^{N_{\mathrm{B},p}-2} \sum_{k=B_b^{\mathrm{u}}}^{B_{b+1}^{\mathrm{l}}} e^{-jk(\Omega-\Omega_\nu)} \\ &\quad + \sum_{k=B_{N_{\mathrm{B},p}-1}^{\mathrm{u}}}^{VN-1} e^{-jk(\Omega-\Omega_\nu)},\ n = 0, \ldots, N-1. \end{aligned}$$

The frequency and the subcarrier index n and ν are represented by $\Omega = 2\pi n/V/N$ and $\Omega_\nu = 2\pi\nu/V/N$, respectively. Note, when only one notch occurs, i.e. $N_{\mathrm{B},p} = 1$, the second term vanishes.

With the known subcarrier spectra, the PB impact on the nth subcarrier can be compensated by subtracting the influences of all other subcarriers with index $\nu \neq n$. The subcarriers outside the OFDM bandwidth are loaded with zeros and can be omitted by ideally low-pass filtering the used OFDM bandwidth. The spectral shape of each subcarrier is also determined by the complex symbol the subcarrier is loaded with. At Rx, this includes the transmitted data symbol as well as the channel influences the subcarrier has experienced. Hence, an estimation of transmitted data symbols $\hat{d}_p[\nu]$ and the estimated fading coefficients $\hat{H}_p[\nu]$ have to be taken into account. The estimation of both data symbols and channel coefficients is addressed in the following two paragraphs. Finally, the OFDM signal $R_p^{\mathrm{comp}}[n]$ after compensating the PB impact on the N relevant subcarriers writes

$$R_p^{\mathrm{comp}}[n] = R_p'[n] - \sum_{\substack{\nu=0 \\ \nu \neq n}}^{N-1} \hat{H}_p[\nu]\hat{d}_p[\nu]S_{p,\nu}[n + N(V-1)/2] \quad n = 0, \ldots, N-1 \quad (7)$$

with $R_p'[n], n = 0, \ldots, N-1$, denoting the ideally low-pass filtered Fourier transform of the Rx signal $r_p'^{\mathrm{ov}}[k]$ after pulse blanking.

C. Estimation of Data Symbols

An estimation of the Tx sequence is derived from the Rx sequence by equalizing, demodulating, and decoding the Rx signal as usual. To obtain improved estimates $\hat{d}_p[\nu], \nu = 0, \ldots, N-1, p = 0, \ldots, P-1$, of the Tx symbols, the decoded bits are encoded and modulated again. ICI is then reconstructed and subtracted from the Rx signal according to (7). In order to improve the reliability of the estimates of the Tx sequence, an iterative structure is introduced as shown in the simplified Rx block diagram in Fig. 3. After the first iteration, estimates of the Tx sequence are derived from the Rx signal, where the impact of ICI has already been partly compensated. With the thus obtained more accurate estimates of the Tx symbols, ICI can be further reduced. The number of required iterations depends on the actual interference conditions and the related number of blanked samples of the OFDM signal. Furthermore, coding reduces the required number of iterations as several bit errors are already corrected at the decoder.

D. Channel Estimation

Estimates of the channel coefficients of all subcarriers and all OFDM symbols are gathered from the channel estimation algorithm usually performed at the OFDM Rx. As an example, pilot-aided linear interpolation is considered as it is intended to be used in L-DACS1 [1]. In order to make channel estimation robust towards interference, the pilot pattern depicted in Fig. 4 has been proposed for L-DACS1. In time direction, the distance between pilot tones is set to five, except for the beginning and the end of a frame. In frequency direction, no regular distance of pilot tones can be given, since they are spread over all OFDM symbols in order to diminish the number of pilot tones, which would be affected if an OFDM symbol coincides with a strong DME pulse. However, the distance of subcarriers which contain pilot tones can be given by four and five at the edge of the spectrum, respectively. These

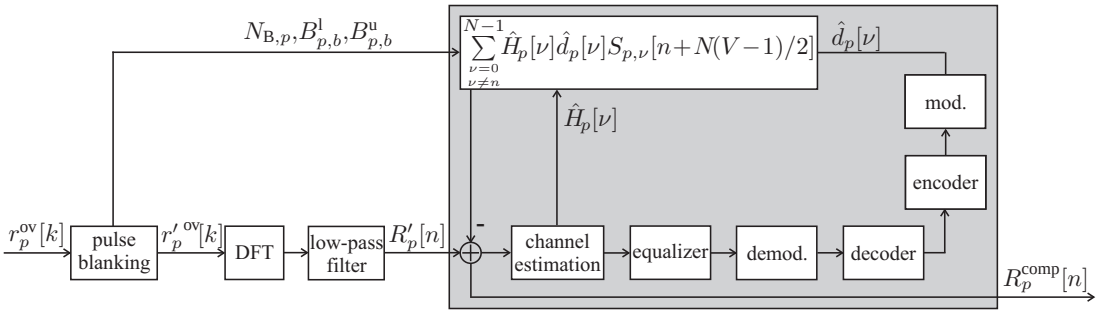

Fig. 3. Simplified block diagram of OFDM Rx with compensation of PB impact.

pilot distances have been chosen to resolve the expected time variance and frequency selectivity of the channel in accordance to the sampling theorem.

The algorithm for channel estimation consists of an interpolation in time direction and a subsequent interpolation in frequency direction. Based on the channel coefficients at pilot positions, e.g. $\tilde{H}_p[\nu]$ and $\tilde{H}_{p+\lambda}[\nu]$, with λ being the distance of two adjacent pilot tones in time direction, the channel coefficients at data positions in between are calculated by

$$\hat{H}_{p+i}[\nu] = \frac{\lambda - i}{\lambda}\tilde{H}_p[\nu] + \frac{i}{\lambda}\tilde{H}_{p+\lambda}[\nu],\ i = 1, \ldots, \lambda - 1. \quad (8)$$

This one-dimensional interpolation is applied to all subcarriers containing pilot tones.

Based on the channel coefficients at pilot positions and the channel coefficients calculated in the first step, the missing channel coefficients on non-pilot subcarriers are calculated in the second step by an one-dimensional interpolation in frequency direction. Eq. (8) also holds for this procedure by simply changing p and ν. In addition, the $\tilde{H}_p[\nu]$ comprise not only channel coefficients at pilot positions, but also channel coefficients at data positions which have been estimated in the first step.

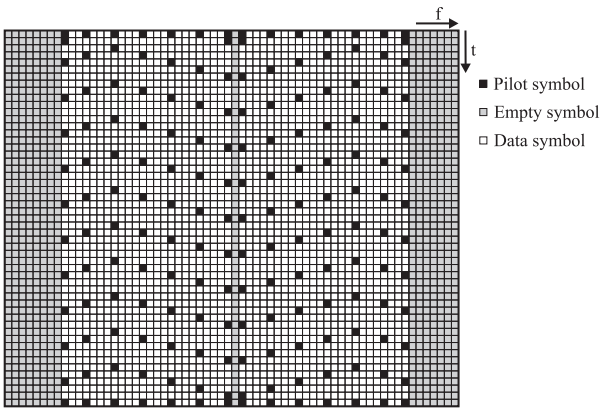

Fig. 4. OFDM frame with pilot symbols.

E. Reconsideration of Threshold for Pulse Blanking

Assuming that ICI is perfectly reduced and the channel is perfectly equalized, the Rx signal comprises the desired OFDM signal, AWGN $N'_p[n]$ slightly modified by PB and equalization, and the interference signal $I'_p[n]$ remaining after PB and equalization and writes

$$R_p^{\mathrm{comp}}[n] = d_{p,n} + N'_p[n] + I'_p[n], \quad n = 0, \ldots, N-1,\ p = 0, \ldots, P-1. \quad (9)$$

The remaining interference signal may impede an accurate estimation of the Tx symbols, in particular with respect to the fact that the influence of the remaining interference cannot be diminished by employing several iterations. A straightforward approach to circumvent this problem is reducing the PB threshold T^{PB} in order to keep the remaining interference as small as possible. Again, the optimal threshold has to be determined, now as a trade-off between the remaining interference power and the impact onto the desired OFDM signal remaining after PB compensation. Hence, the optimization of the threshold is revisited taking into account the compensation of the PB impact. Again, the SINR after PB and PB compensation serves as optimization criterion.

V. Simulation Results

For evaluating the performance of the proposed compensation algorithms simulations are carried out taking into account realistic interference conditions. The victim OFDM Rx is located in the center of the area with the highest density of DME stations, i.e. at Paris, Charles-de-Gaulles airport. To reproduce interference conditions at an en-route flight the victim OFDM Rx is positioned at an altitude of 15 km. The peak interference power originating from all surrounding DME/TACAN stations on the ground is determined via simple link budget calculations, taking into account free space loss and antenna patterns dependent on elevation angles. Typical interference conditions are observed when the OFDM system is operated at 994.5 MHz, for example. In the channels at $\pm$500 kHz offset, four TACAN stations with power and duty cycle as listed in Tab. I are observed. Note, in this part of the L-band, only interference from DME ground stations has to be considered, since no DME airborne stations are operated in this range.

The basic parameters of the OFDM system that is operated in the spectral gap between two adjacent DME channels are listed in Tab. II. For coding and modulation, a (133,171)

TABLE I
EN-ROUTE INTERFERENCE SCENARIO.

Station	Frequency	Interference power at victim Rx input	Pulse rate
TACAN	994 MHz	-72.4 dBm	3600 ppps
TACAN	994 MHz	-74.0 dBm	3600 ppps
TACAN	994 MHz	-88.2 dBm	3600 ppps
OFDM	994.5 MHz		
TACAN	995 MHz	-67.9 dBm	3600 ppps

convolutional code with rate 1/2 and QPSK modulation are applied, respectively. Propagation through the radio channel is modelled by an appropriate en-route channel model taking into account a strong line-of-sight path, Doppler frequencies of up to 1.25 kHz, and two delayed paths. Note, although the maximum path delay does not exceed 15 μs, the length of the cyclic prefix is much longer. The additional samples are employed in the OFDM transmitter for Tx windowing in order to reduce out-of-band radiation.

TABLE II
OFDM SYSTEM PARAMETERS.

Parameter	**Value**
Used bandwidth	510.416 kHz = 49 · 10.416 kHz
Subcarrier spacing	10.416 kHz
FFT length	64
Sampling rate	666.666 kHz
OFDM symbol duration	96 μs
Cyclic prefix	24 μs
Total OFDM symbol duration	120 μs
OFDM symbols per frame	53
OFDM frame duration	6.36 ms

In Fig. 5, the bit error rate (BER) vs. signal-to-noise ratio (SNR) is shown for the case of perfect channel estimation. The large gap between the performance with and without interference given as reference motivates the need for mitigating the impact of interference. When considering PB with threshold optimized without taking into account the PB compensation, i.e. $T^{\text{PB}} = 2.25$, performance is rather poor. Note, the PB threshold is given relative to the amplitude of the desired OFDM signal which is normalized to 1. With PB itself, the impact of interference is reduced by only 1.7 dB at BER $= 10^{-4}$. Compensating the PB impact perfectly, i.e. based on the known Tx sequence, yields a considerable performance improvement. However, the gap to the interference-free case still is as high as 2.4 dB. A comparison to the performance of perfect PB compensation without interference shows that the poor performance can be explained by the high remaining interference power, hence suggesting a reduction of T^{PB}.

When optimizing the PB threshold taking into account the subsequent compensation, the threshold is significantly smaller, i.e. $T^{\text{PB}} = 1.25$. This results in even worse performance when only PB is applied since the OFDM signal is derogated significantly. However, when the impact of PB is compensated afterwards, performance improves and the impact of interference can be reduced such that the interference-free case is approached by 1.6 dB in the ideal case. The small gap to the performance of ideal compensation without interference shows that only a slight fraction of interference remains after PB compensation. The remaining gap to the interference-free case is explained by the SNR loss induced when erasing a certain fraction of the signal and cannot be compensated. At the considered SNR, on the average, 23.75% of the samples of the OFDM signal are blanked, which results in an SNR loss of 1.2 dB.

With PB compensation based on an estimation of the Tx sequence, nearly the same performance as in the ideal case is achieved for SNR >5 dB. For these results, only one iteration is sufficient and no further improvements are achieved with additional iterations.

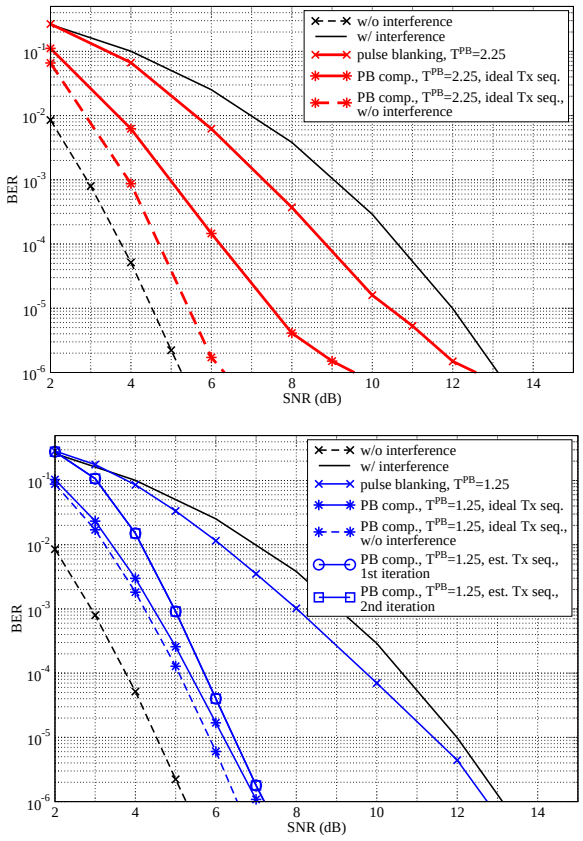

Fig. 5. BER after compensation of pulse blanking impact, $T^{\text{PB}} = 2.25$ (above), $T^{\text{PB}} = 1.25$ (below), en-route interference scenario, perfect channel estimation.

In the case of perfect channel knowledge, i.e. $\hat{H}_p[\nu] = H_p[\nu]$, the channel coefficients have no influence on the iterative gain of our scheme. Taking into account real channel estimation, performance is expected to be worse than with perfect channel estimation. However, the estimates of the channel coefficients $\hat{H}_p[\nu]$ are expected to improve with increasing number of iterations. The BER curves in Fig. 6 validate this assumption. When iterating three times, the SNR improves by 0.7 dB at BER $= 10^{-4}$ compared to one iteration. As has been shown in Fig. 5 for the case of perfect channel

knowledge, even a second iteration had no further beneficial influence. It is also remarkable that for SNR $>$ 7.5 dB, the deteriorating influence of real data estimation compared to perfect knowledge of the data symbols is outperformed by the iterative gain of the channel estimation. Due to this iterative gain of the channel estimation, the interference-free case is approached by 2.8 dB which is only 1.2 dB less than in the case with perfect channel estimation. Additional iterations do not lead to further performance improvements.

Fig. 7 clarifies the influence of the algorithm on the channel estimation in terms of the mean square error (MSE) of the estimated channel coefficients compared to perfect known channel coefficients vs. SNR. For SNR $>$ 9.6 dB the channel estimation when PB with $T^{\mathrm{PB}} = 1.25$ is applied is even worse compared to the case without PB, hence indicating the corruptive influence of PB itself onto all subcarriers. When compensating the influence of PB only by one iteration, the MSE of the channel estimation is already considerably reduced. Increasing the number of iterations leads only to little further improvement of the channel estimation. This is in accordance to the BER improvement observed in Fig. 6.

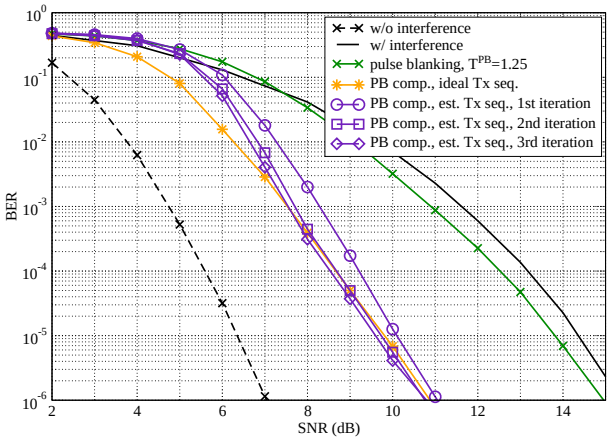

Fig. 6. BER after compensation of pulse blanking impact, en-route interference scenario, real channel estimation, $T^{\mathrm{PB}} = 1.25$.

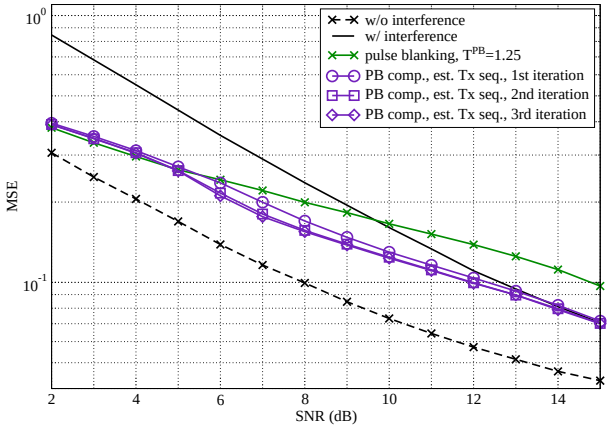

Fig. 7. MSE of channel estimation, $T^{\mathrm{PB}} = 1.25$.

VI. Conclusion

When mitigating the impact of pulsed interference in OFDM systems by means of pulse blanking, only moderate improvements are achieved, since pulse blanking substantially impairs the useful OFDM signal. To improve the performance of pulse blanking in OFDM systems, the compensation of the impact of pulse blanking on the useful signal is proposed. ICI induced by pulse blanking is subtracted based on a reconstruction of the subcarrier spectra after pulse blanking and an estimation of the Tx data symbols and the channel coefficients of each subcarrier. The achieved improvements allow for blanking even more samples and further reducing the remaining interference power while improving overall performance. Assuming perfect channel estimation, it is shown that the impact of remaining interference is mitigated nearly completely. The impact of pulse blanking is reduced to an SNR loss resulting from erasing a certain fraction of the OFDM signal. Taking real channel estimation into account, similar observations are made. Despite an initial performance degradation compared to the ideal case, the inaccuracies in the estimation of Tx data symbols and channel coefficients diminish and performance improves with increasing number of iterations. Due to the iterative gain, the interference-free case is approached by 2.8 dB after three iterations. Compared to the ideal case, this means a performance degradation of only 1.2 dB.

In future work, the estimation of the data symbols can be improved, e.g. by using soft values at the decoder output and weighting the estimated and subtracted data symbols according to their reliability. Other approaches for channel estimation may lead further performance improvements. In addition, a joint approach for estimation of channel coefficients and Tx data can be pursued as it has already been proposed for jointly estimating carrier frequency offsets and channel coefficients in OFDMA systems.

References

[1] M. Schnell, S. Brandes, S. Gligorevic, M. Walter, C. Rihacek, M. Sajatovic, and B. Haindl, "Interference Mitigation for Broadband L-DACS," in *27th Digital Avionics Systems Conference (DASC)*, St. Paul, MN, USA, October 2008, pp. 2.B.2–1 – 2.B.2–12.

[2] G. X. Gao, "DME/TACAN Interference and its Mitigation in L5/E5 Bands," in *ION Institute of Navigation Global Navigation Satellite Systems Conference*, Fort Worth, TX, USA, September 2007.

[3] S. V. Zhidkov, "Analysis and Comparison of Several Simple Impulsive Noise Mitigation Schemes for OFDM Receivers," *IEEE Transactions on Communications*, vol. 56, no. 1, pp. 5–9, January 2008.

[4] P. Banelli and S. Cacopardi, "Theoretical analysis and performance of OFDM signals in nonlinear AWGN channels," *IEEE Transactions on Communications*, vol. 48, no. 3, pp. 430–441, March 2000.

[5] S. Brandes and M. Schnell, "Interference Mitigation for the Future Aeronautical L-Band Communication System," accepted for publication at 7th International Workshop on Multi-Carrier Systems & Solutions (MC-SS 2009), Herrsching, Germany, May 2009.

[6] R. Fantacci, D. Marabissi, and S. Papini, "Multiuser interference cancellation receivers for OFDMA uplink communications with carrier frequency offset," in *Proc. of IEEE Global Telecommunications Conference (Globecom'04)*, Dallas, TX, USA, November 2004, pp. 7081–7085.